Optimal Sensor Fusion using $\mathcal{H}_\infty$ methods

Synthesizing Complementary Filters for Active Seismic Noise Isolation Systems in KAGRA

Terrence T.L. Tsang on behalf of the KAGRA Collaboration

The Chinese University of Hong Kong. Email: ttltsang@link.cuhk.edu.hk

Introduction

Ground-based gravitational-wave detectors require active control systems at low frequency to attenuate seismic noise induced displacement for the interferometer main optics. Such active isolation systems utilize local displacement sensors for feedback control. While the control performance of suspensions is limited by the sensors, it's desirable for sensors to be as low-noise as possible. In this work, we will describe a sensor fusion architecture that combines two sensors with different noise characteristics to obtain a virtual "super sensor" that has overall better noise performance.

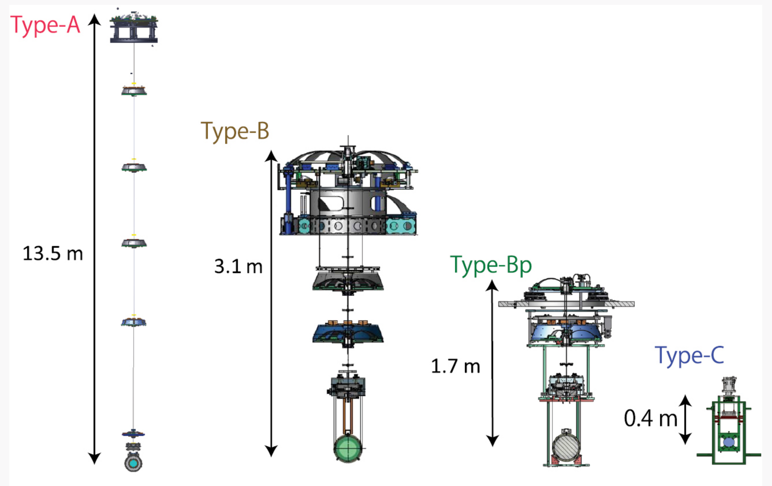

Figure 1: Type-A suspensions: input/end test masses, Type-B suspensions: beamsplitter and signal-recycling mirrors, Type-Bp suspensions: power-recycling mirrors, and Type-C suspensions: input/output mode cleaners [1].

We apply the so-called "complementary filters" on the sensors and the signals are then summed to become the readout of the super sensor. Complementary filter designs were proposed previously [2, 3, 4], but they were not suboptimal. More importantly, besides heuristics, it was not clear how exactly the filter shapes were constrained according to the sensor noises in question. Here, we propose to formulate the complementary filter problem as an $\mathcal{H}_\infty$ optimization problem and synthesize the filters, which optimally combine the sensors, using $\mathcal{H}_\infty$ method.

Methodology

Fig. 2 shows a the block diagram typical two-sensor sensor fusion configuration using complementary filters. The two sensors are each filtered with filters $H_1(s)$ and $H_2(s)$ respectively. We required that the super sensor measuring the same signal that the two sensors are reading, so the filters must be complementary, i.e.

$$H_1(s) + H_2(s) = 1\,. \tag{1}$$

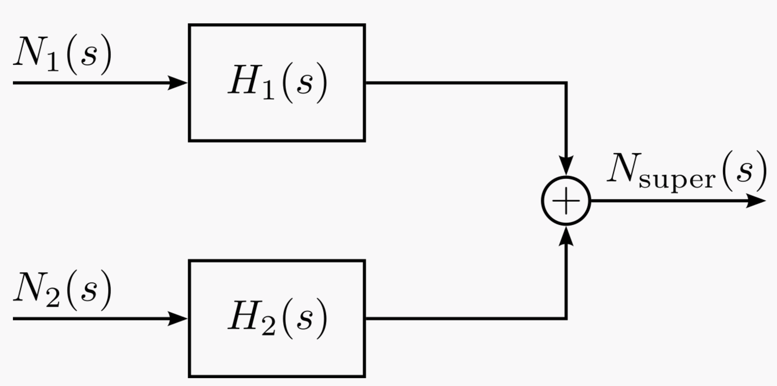

Figure 2: Two-sensor complementary filter configuration.

The super sensor noise then reads

$$N_{\mathrm{super}}(s) = H_1(s)N_1(s) + H_2(s)N_2(s)\,. \tag{2}$$

So, the goal is to design the complementary filters $H_1(s)$ and $H_2(s)$ such that $N_{\mathrm{super}}(s)$ is minimized in some sense, or exhibit desirable noise characteristics.

This is where $\mathcal{H}_\infty$ method comes in. $\mathcal{H}_\infty$ method is used to synthesize regulator for feedback systems but is recently proposed for synthesizing complementary filters with frequency-dependent specification [5]. And, It was shown that the method successfully reproduced one of the complementary filters at LIGO [6] using the same specifications. To use $\mathcal{H}_\infty$ method, the input-output system is first represented in the generalized plant representation as shown in Fig. 3.

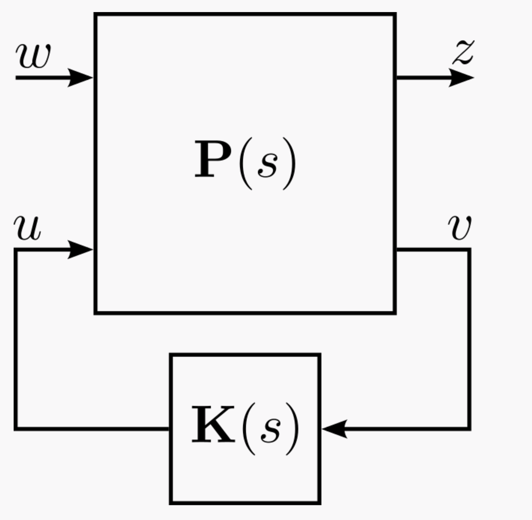

Figure 3: Generalized Plant Represenation

In the figure, w are the inputs, z are the error signals to be minimized, u are the manipulated variables, v are the measurement signals, $\mathbf{P}(s)$ is the open loop plant, and $\mathbf{K}(s)$ is the closed-loop regulator. The close-loop response can be written as

$$z = \mathbf{G}(s)w\,, \tag{3}$$

where $\mathbf{G}(s)$ is the transfer function matrix from the inputs w to the errors z.

Methodology (cont.)

$\mathcal{H}_\infty$ synthesis will then generate a regulator $\mathbf{K}_\infty(s)$, which minimizes the $\mathcal{H}_\infty$ norm of the closed-loop transfer function $\mathbf{G}(s)$. The definition of $\mathcal{H}_\infty$ norm is more involved and its discussion is skipped for brevity.

Consider the generalized plant architecture as shown in Fig. 4, which is a slight modification from that of [5]. Here, Φ_1 and Φ_2 are some uncorrelated stochastic processes with unit magnitude. $\hat{N}_1(s)$ and $\hat{N}_2(s)$ are transfer function models of the noises N_1 and N_2. $W_1(s)$ and $W_2(s)$ are some weighting functions, which can be used to specify the (inverse) frequency-dependent specification of the sensing noises N_1 and N_2 respectively.

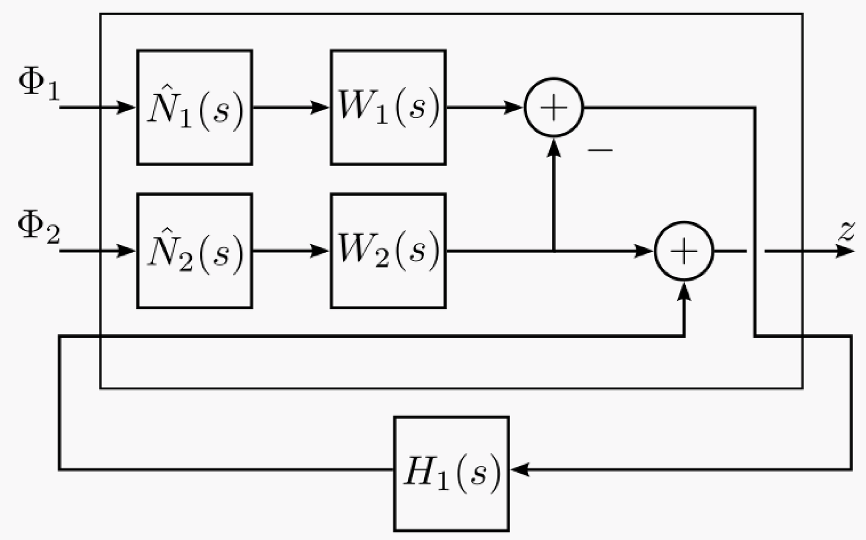

Figure 4: Generalized plant representation for complementary filter synthesis.

Minimizing the $\mathcal{H}_\infty$ norm of this plant will give optimal filters $H_1(s)$ and $H_2(s) \equiv 1 - H_1(s)$ that best filter the noises N_1 and N_2 according to the specifications. It follows that if we set $W_1(s) = 1/\hat{N}_2(s)$ and $W_2(s) = 1/\hat{N}_1(s)$, the requirements of N_1 is set to N_2 when $N_1 \gg N_2$, and vice versa. These weights are reasonable specifications if there's no specific requirements for the sensing noises because over-suppressing one of the noises is not useful as there exists a lower bound defined by the one of N_1 or N_2.

Results

In this section, the proposed method will be exemplified with sensing noises taken from the preisolator (PI) of the signal-recycling mirror in KAGRA. We will also compare the performance of the complementary filters designed using the method in [2, 3] and using the proposed method. The amplitude spectral densities (ASDs) of the sensing noises $N_1(s)$ and $N_2(s)$ and the transfer function models $\hat{N}_1(s)$ and $\hat{N}_2(s)$ are shown in Fig. 5. Here, N_1 denotes quadrature sum of the relative displacement sensor (LVDT) self-noise and the mean seismic noise at KAGRA taken from [7], whereas N_2 is the geophone self-noise.

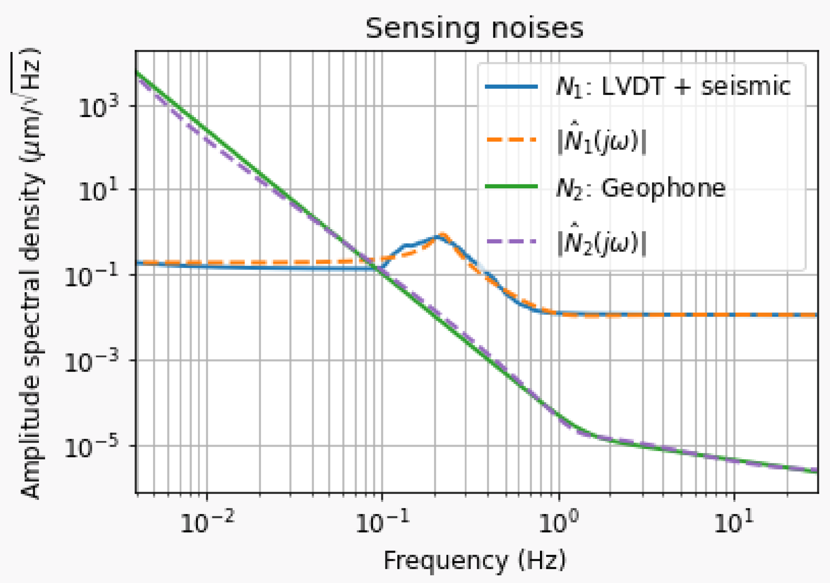

Figure 5: Sensing noises of the SRM PI sensors.

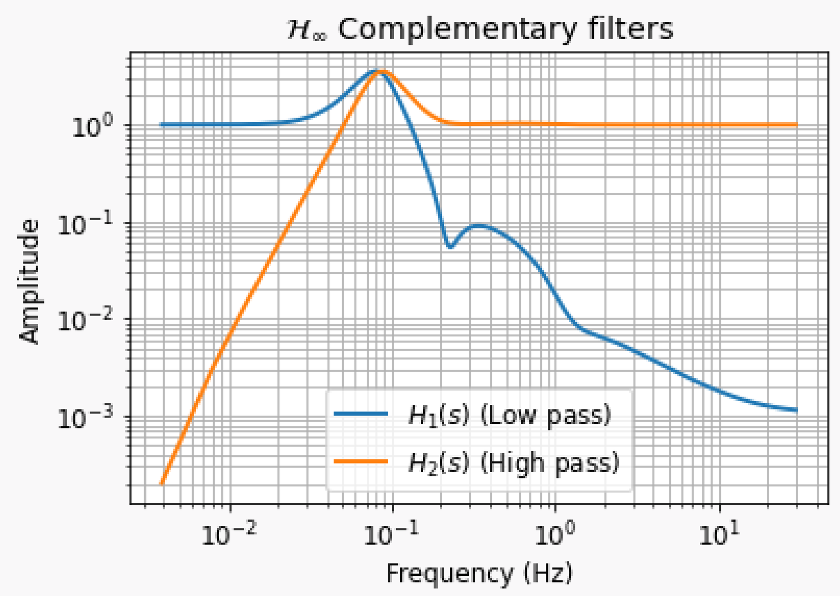

Figure 6: Filters synthesized using $\mathcal{H}_\infty$ method.

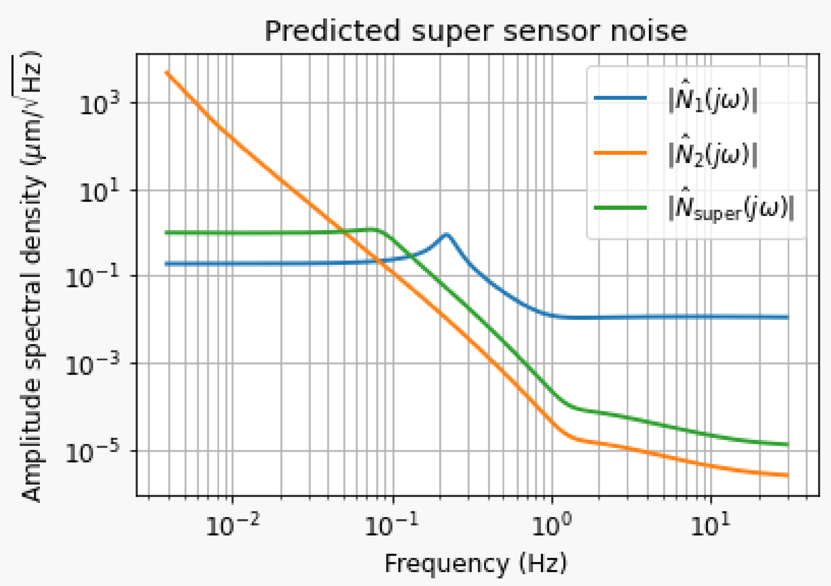

Figure 7: Predicted super sensor noise

Using the noise models $\hat{N}_1(s)$ and $\hat{N}_2(s)$, complementary filters were synthesized using $\mathcal{H}_\infty$ method as described in the methodology section. The resulting complementary filters are shown in Fig. 6.

Results

Fig. 7 shows the predicted super sensor noise defined by

$$\left|\hat{N}_{\mathrm{super}}(j\omega)\right| = \left[|H_1(j\omega)|^2\left|\hat{N}_1(j\omega)\right|^2 + |H_2(j\omega)|^2\left|\hat{N}_2(j\omega)\right|^2\right]^{\frac{1}{2}}\,. \tag{4}$$

As can be seen, the super sensor noise here follows the shape of the lower bound of the sensing noises at all frequencies, which would indicate that the order of roll-off is critical at all frequencies.

In Fig. 8, we compare noise performance of the complementary filters from [2], [3], and the proposed method, which are denoted $N_{\mathrm{super,\,1}}$, $N_{\mathrm{super,\,2}}$, and $N_{\mathrm{super},\mathcal{H}_\infty}$ respectively. The super sensor noises were calculated directly using the noises N_1 and N_2, instead of the transfer function models, as shown in Fig. 5.

The cross-over frequency of the filters in [2, 3] were set to be the cross-over frequency of the sensing noises in Fig. 5, which is 0.0898 Hz in this case. This is the recommended way as discussed in [2]. As can be seen, the amplitude spectral density of the super sensor noise from $\mathcal{H}_\infty$ filters are on par, if not lower, compared to the other two below 0.4 Hz and is slightly higher above that. The shape of $N_{\mathrm{super},\mathcal{H}_\infty}$ at higher frequencies still follows that of the lower bound, which again, indicating that the sensing noises are critically roll-offed.

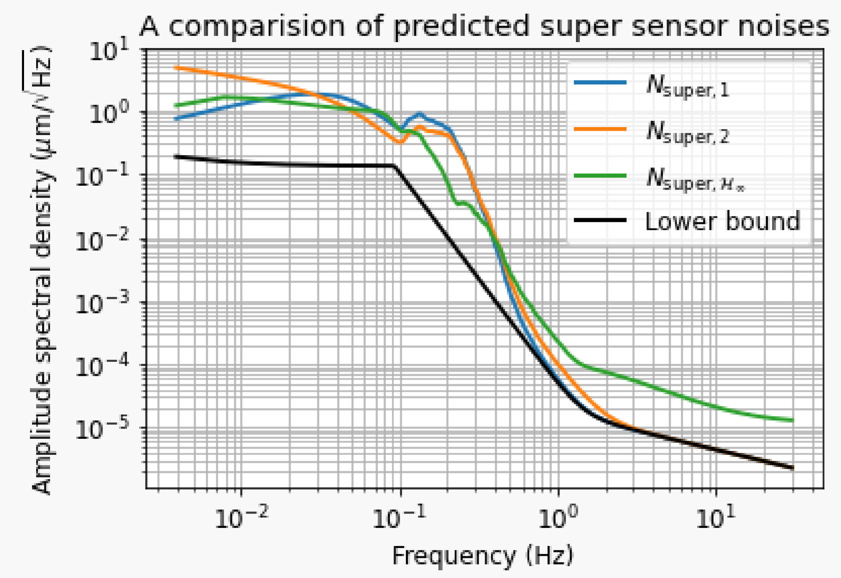

Figure 8: Comparison between the super sensor noises predicted using filter design from [2, 3] and the proposed method.

A few metrics are compared in table. 1, i.e. the root mean square (RMS) value of the super sensor noise, band-limited RMS around the microseism band (0.1-0.5 Hz), ASD at 10 Hz (beginning of the detection band).

	RMS (μm)	RMS (0.1-0.5 Hz) (μm)	ASD (10Hz) (μm/$\sqrt{\mathrm{Hz}}$)
$N_{\mathrm{super,\,1}}$	0.5895	0.2400	4.443e-6
$N_{\mathrm{super,\,2}}$	0.4726	0.1650	4.443e-6
$N_{\mathrm{super},\mathcal{H}_\infty}$	0.3631	0.1041	2.087e-5
Lower bound	0.0462	0.01422	4.443e-6

Table 1: RMS, bound-limited RMS, and ASD value at 10 Hz of the super sensor noises predicted using filter design from [2, 3] and the proposed method.

Conclusion

References

[1] T. Akutsu et al.
Vibration isolation systems for the beam splitter and signal recycling mirrors of the KAGRA gravitational wave detector.
Class. Quant. Grav., 38(6):065011, 2021.

[2] T. Sekiguchi.
Study of Low Frequency Vibration Isolation System for Large Scale Gravitational Wave Detectors.
PhD thesis, Tokyo U., 2016.

[3] Joris Vincent van Heijningen.
Turn up the bass! Low-frequency performance improvement of seismic attenuation systems and vibration sensors for next generation gravitational wave detectors.
PhD thesis, Vrije U., Amsterdam, 2018.

[4] Lucia Trozzo.
Low Frequency Optimization and Performance of Advanced Virgo Seismic Isolation System.